Center of pressure displacement due to graded controlled perturbations to the trunk in standing subjects: the force–impulse paradigm

DOI:10.1007/s00421-021-04844-9

(Article begins on next page)

Original Article

Center of pressure displacement due to graded controlled perturbations to the trunk in standing subjects: the force-impulse paradigm

Maria Paterna[1], Zeevi Dvir[2], Carlo De Benedictis[1], Daniela Maffiodo[1], Walter Franco[1], Carlo Ferraresi[1], Silvestro Roatta[3*]

[1] Dept. of Mechanical and Aerospace Engineering, Politecnico di Torino, Torino, Italy
[2] Dept. of Physical Therapy, Faculty of Medicine, Tel Aviv University, Tel Aviv, Israel
[3] Dept. of Neuroscience, University of Torino, Torino, Italy

*Correspondence to:
Silvestro Roatta
Dip. di Neuroscienze, Università di Torino
c.so Raffaello 30, 10125, Torino, Italy
tel +39 011 6708164
e-mail: silvestro.roatta@unito.it
ORCID: 0000-0001-7370-2271

ABSTRACT

Purpose: Many studies have investigated postural reactions (PR) to body-delivered perturbations. However, attention has been focused on the descriptive variables of the PR rather than on the characterization of the perturbation. This study aimed to test the hypothesis that the impulse rather than the force magnitude of the perturbation mostly affects the PR in terms of displacement of the center of foot pressure (ΔCoP).

Methods: Fourteen healthy young adults (7 males and 7 females) received two series of 20 perturbations, delivered to the back in the anterior direction, at mid-scapular level, while standing on a force platform. In one series, the perturbations had the same force magnitude (40 N) but different impulse (range: 2-10 Ns). In the other series the perturbations had the same impulse (5 Ns) but different force magnitude (20-100 N). A simple model of postural control restricted to the sagittal plane was also developed.

Results: The results showed that ΔCoP and impulse were highly correlated (on average: $r=0.96$) while the correlation ΔCoP–force magnitude was poor ($r=0.48$) and not statistically significant in most subjects. The normalized response, $\Delta CoP_n=\Delta CoP/I$, was independent of the perturbation magnitude in a wide range of force amplitude and impulse and exhibited good repeatability across different sets of stimuli (on average: ICC=0.88). These results were confirmed by simulations.

Conclusion: The present findings support the concept that the magnitude of the applied force alone is a poor descriptor of trunk-delivered perturbations and suggest that the impulse should be considered instead.

Keywords: Postural reaction; perturbation; force; impulse; center of pressure; balance control.

1. INTRODUCTION

Research on postural reactions (PR) has employed a variety of perturbation techniques intended to simulate in laboratory conditions the events that challenge the body equilibrium in real life. Two distinct approaches have been followed: imparting the perturbation i) to the base of support by sliding or tilting the platform (Schmidt et al. 2015; Grassi et al. 2017; Robbins et al. 2017) or ii) directly to the upper body. These two perturbation modes elicit fundamentally different PR (Bortolami et al. 2003; Colebatch et al. 2016; Chen et al. 2017) and thus are both worth to be pursued. However, while the moving platform is easily described and standardized in terms of extent and speed of displacement and rotation, description and quantification of upper body perturbation are more difficult. Direct body perturbation has been achieved in the most disparate of ways. Some devices were based on imparting a pull force to the body by the sudden release of a weight connected to the body via a cable (Martinelli et al. 2015; Maaswinkel et al. 2016; Azzi et al. 2017) or employing electric actuators (Pidcoe and Rogers 1998; Sturnieks et al. 2013; Fujimoto et al. 2015; Robert et al. 2018), which, however, alter the subject's resting posture, thus potentially affecting the overall PR. Others are based on the application of a push force imparted manually by pushing the subject with the hands (Colebatch et al. 2016), or by releasing a pendulum which hits the body at shoulder level (Kim et al. 2012), or by the action of a hand-held device which records the force profile during contact with the subject (Kim et al. 2009; Pasman et al. 2019; Dvir et al. 2020). In most cases little attention was devoted to the characterization of the perturbation and the relation between the magnitude of the perturbation and the postural response, focusing instead on the factors affecting CoP steadiness (Martinelli et al. 2015; Azzi et al. 2017; Grassi et al. 2017) or its association with the risk of falling (Sturnieks et al. 2013; Fujimoto et al. 2015). However, the precise identification of the input variable that better correlates with the CoP response could facilitate the interpretation of the results and the design of appropriate postural tests. Significantly, it could enhance testing of patients affected with disorders in which the normal PR may be compromised (Grassi et al. 2017; Colebatch and Govender 2019).

Although it is generally acknowledged that, within the boundaries of stability, the greater the magnitude of the perturbation the greater is the PR (Diener et al. 1988; Kim et al. 2009; Azzi et al. 2017; Forghani et al. 2017; Teixeira et al. 2019), very few studies investigated this relation with upper body-directed perturbation. Kim et al (2009) evidenced a positive correlation between the peak force of a body-directed push perturbation and the displacement of the center of pressure (CoP). However, by exploring specifically this facet of PR, we have recently observed that in young men, the magnitude of the CoP response, in terms of its displacement, was better correlated with the impulse than with the peak force of the postural perturbation (Dvir et al. 2020). On one hand, it may seem obvious that the magnitude of the perturbation cannot be simply characterized by the magnitude of the force but should also depend on the duration of the push. On the other hand, the impulse, indeed defined as the integral of force over time, has surprisingly not gained much consideration in the literature, even though it corresponds to the momentum transferred to the body. As such, it is directly related to the change in speed of the body and thus to the energy transmitted by the perturbation.

The preliminary observation presented in Dvir et al.(2020) did not provide a clear-cut indication with regard to the impulse vs. force paradigm, possibly because of data dispersion. The postural perturbations were manually delivered, with high intra- and inter- subject variability, in terms of force amplitude, duration and impulse. This could have accounted for the intra-subject variability of the response and the low Pearson correlation coefficient values observed in some subjects.

Aim of the present study is to reinvestigate the hypothesis that the CoP displacement due to trunk-directed push perturbations is linearly correlated with the magnitude of the impulse and not with the force magnitude, by means of a renewed experimental approach and model simulations. In order to reduce the variability in the magnitude of the perturbations a novel pneumo-tronic device was developed, capable of imparting simultaneous force- and duration-controlled perturbations (Ferraresi et al. 2020a, b; Maffiodo et al. 2020). In addition, the experimental results are discussed and compared with a simulation of the CoP response based on a simple single-link inverted pendulum model.

2. METHODS

2.1 Experimental test

2.1.1 Subjects

A group of 14 healthy young adults, 7 females (mean(SD) age: 22.7(1.7)years; height: 1.62(0.05)m; weight: 54.0(4.2)kg; BMI: 20.7(1.5)kg/m^2) and 7 males (mean(SD) age: 23.1(2.7)years; height: 1.78(0.11)m; weight: 70.3(6.0)kg; BMI: 22.3(1.6)kg/m^2), was recruited from the student population at the Politecnico di Torino. Exclusion criteria included: recent lower extremity injury and/or fracture

(< 1 year), previous reconstructive surgery in the lower extremity and balance deficits. All subjects provided written informed consent to participate in this study which was approved by the institutional review board of the University of Torino (Prot. n. 380583).

2.1.2 Task and instrumentation

The experimental task consisted of recovering balance following impulsive perturbations applied to the trunk in the anterior direction while standing on a force platform.

The force platform, a modified Shekel (Beit Keshet, Israel) device, was made up of a still plate (52x36 cm) which was supported by 4 uniaxial load cells (TEDEA, Israel, model 1042, rated capacity 100 kgf), mounted on a base plate. The perturbation was applied by a pneumo-tronic perturbator designed and constructed at the Dept. of Mechanical and Aerospace Engineering at the Politecnico di Torino. The instrument is shown in Fig. 1A and was described in detail in another publication (Ferraresi et al. 2020b). The closed-loop force feedback design, based on the continuous monitoring of the perturbation force provided by a load cell positioned in series with the tip of the perturbator, allows for the regulation of the precise intensity and duration of the stimulus delivered to the subject, irrespective of the mechanical compliance of the operator (Ferraresi et al. 2020b).

2.1.3 Procedure

During the test, the subjects stood barefoot on the force platform with the feet at pelvic distance and with vision unobstructed. Subjects were asked to assume a normal-relaxed stance and they were instructed to respond naturally. The feet locations were traced onto the platform surface to ensure consistent initial foot placement across test sessions for each participant. The operator stood behind the subject holding the perturbator while the interface was maintained at a distance of about 2 cm from the subject's back (Fig. 1B). Immediately before the starting of the test, participants were familiarized with the procedure by receiving few perturbations. The perturbations were delivered to the trunk always at inter-scapular level (IS), given that, at this site, more reproducible responses could be obtained, compared to lumbar level (Dvir et al. 2020).

The test comprised two series, with a break of 5 min in between. In one series, namely the constant-force series, the perturbations had the same force magnitude (40 N), but different impulse values (2 Ns; 4 Ns; 6 Ns; 10 Ns). In the other series, namely the constant-impulse series, the perturbations had the same impulse (5 Ns) but different force magnitude (20 N; 40 N; 60 N; 100 N). Based on our previous experience, we operated in a range of values large enough to elicit a clearly detectable response and small enough to exclude a step response. The values of 40 N and 5 Ns were arbitrarily chosen as intermediate values within that range. The average force perturbation profiles, for each condition, are shown in Fig. 2.

In each series, the subjects received a total of 20 perturbations, 5 for each force profile mentioned above. The sequences of perturbations, each one including 5 equal stimuli, were provided in random order. An inter-perturbation pause of at least 10 s was allowed for returning to relaxed stance. The order of the 2 series was randomized as well. A typical testing session lasted about 20 minutes.

2.1.4 Data processing

Data were extracted and processed with custom routines developed in MATLAB_R2019b®. The force signal was acquired at 1000 Hz and digitally low-pass filtered using a dual-pass 8^{th} order Butterworth filter with a cut-off frequency of 200 Hz. The actual magnitude of the perturbation was characterized in terms of:

- Force Amplitude (in N): the average force at the plateau. The start and the end of the plateau were automatically detected as the time instants at which the force signal crossed a threshold equal to 95% of the intended force magnitude (see Fig. 3).
- Impulse (in Ns): the integral of force computed over the time interval in which the force is greater than 0.5 N.

The ground reaction forces were acquired at 1000 Hz and were used to calculate the coordinates of the CoP. Both coordinates were digitally low-pass filtered with a dual-pass 8^{th} order Butterworth filter with a cut-off frequency of 20 Hz. The postural response, ΔCoP, was computed as the maximum CoP displacement, observed within 2 s from the perturbation. The displacement (in cm) is calculated from the average resting position, calculated over the 3 s preceding the perturbation.

2.1.5 Statistical Analysis

All statistical procedures were conducted using MATLAB_R2019b®.

Possible differences in impulse and force amplitude among the different perturbation types were analyzed through a Friedman test with grouping factor impulse and force amplitude for the constant-force and constant-impulse series, respectively.

Pearson's correlation coefficient (r) was used to assess the relationship between ΔCoP and the perturbation. The Fisher's Z transform was used to estimate an average correlation coefficient over all subjects. Pearson's coefficient was also calculated to evaluate the relationship between the postural response and the physical characteristics of the subjects. The Friedman's test was used to determine whether the impulse or force amplitude affect the CoP displacement.

Intraclass correlation coefficients ($ICC_{3,k}$), based on a mean rating ($k = 5$), absolute agreement, 2-ways mixed effects model were derived to quantify the reliability of the CoP response among different stimulus magnitudes while the coefficient of variation (CoV) was used to assess the variability of the responses to the same perturbation type. In order to evaluate whether general postural adjustments in anticipation of back perturbations took place during the test, changes in resting CoP were assessed within each session (comparing the beginning and the end of each experimental session, average CoP computed 30-s intervals with no perturbations; Wilcoxon Signed Rank Test) as well as within each of the 8 sequences of stimuli of the same type (comparing the 3-s CoP baseline preceding the first stimulus and the last one of the sequence; Wilcoxon Signed Rank Tests, with Bonferroni correction).

Data in the text are expressed as mean ± standard deviation.

2.2 Single-link inverted pendulum models

The human body orthostatic position perturbed with low entity disturbances occurring in the sagittal plane can be schematized by means of an inverse pendulum model (Winter et al. 1998). The basic scheme, implemented in MATLAB® Simulink® environment, represents the body as a rigid link having a single rotational degree of freedom (DoF) about the ankle joint (Fig. 4). For small oscillations of the body θ, the linearization of the model yields the following equations:

$$\tau + mgd\theta - md^2\frac{d^2\theta}{dt^2} - I\frac{d^2\theta}{dt^2} + F_e h_F = 0 \quad (1)$$

$$CoP = \frac{-\tau - R_x h}{mg} \quad (2)$$

where τ is the correcting torque at the ankle, m is the body mass, g is the gravitational acceleration, d is the distance between ankle joint and the center of mass (CoM), I is the rotational inertia of the body about the CoM, h_F is the distance between ankle joint and the point of application of the perturbation force F_e, CoP is the center of pressure position, R_x is the horizontal component of the ground reaction force, h is the height of ankle joint with respect to the fixed base of support.

Although simplified models of balance control can focus on muscle stiffness alone as the main tool to achieve stabilization in quiet standing, it is well known that such passive behavior is generally not sufficient to ensure stability (Morasso et al. 1999), especially when significant external disturbances are considered. For this reason, the correcting torque at the ankle τ has been modeled as the sum of a passive and an active contribution. The passive contribution is related to the visco-elastic behavior of human tissues and is proportional to both the deformation θ and the rate of deformation $\dot{\theta}$ of the joint (Engelhart et al. 2015), whereas the active contribution depends on the neuromuscular control managed by the central nervous system and can be modeled as a delayed PD (Proportional-Derivative) action (Van Der Kooij et al. 2005). In particular, the output of the controller, i.e., the active torque at the ankle, is aimed at minimizing the error θ, i.e., the current angular displacement from the initial standing position (θ=0). The information about the current angular displacement is fed to the controller by noisy and delayed sensory feedback. Thus, a constant transmission delay was introduced as the latency between the variation of θ and the generation of the reflex active torque (Goodworth and Peterka 2018), and an additive pink noise was introduced to account for the limitations of the sensory system (Van Der Kooij and Peterka 2011; Boonstra et al. 2013; Goodworth and Peterka 2018). Proportional and derivative gains of the PD control model then need to be identified, to match the characteristics of a given subject and to achieve stability. (Van Der Kooij et al. 2005; Van Der Kooij and Peterka 2011; Goodworth and Peterka 2018).

With the limited aim of investigating the theoretical dependence of the CoP response to force and impulse of the perturbation, the model was configured as follows: 1) anthropometric parameters were set equal to average values computed over the participants to the experimental study (with reference to Fig. 4: m = 62 kg, l = 1.70 m, h = 0.1 m, d = 0.6l, $I = ml^2/12$, h_F = 1.2 m); 2) the coefficients of the passive response were set according to the literature (Engelhart et al. 2015); 3) the latency between the generation of the active torque and the variation of θ was set to the constant value of 90 ms, according to the literature (Goodworth and Peterka

2018); 4) active control parameters and noise level were estimated by an iterative least-squares fitting used to match the simulation with the average experimental postural response.

The CoP response to a given perturbation was obtained from the average of 5 distinct simulations, thus accounting for the variability introduced by sensory noise.

3. RESULTS

3.1 Results of the experimental trials

A representative recording of a single perturbation along with the postural response is shown in Fig. 3.

The actual magnitudes for the different experimental perturbation types are shown in Fig. 5 for the two series. In the constant-force series, the perturbator delivered stimuli with different impulses and with similar force amplitude values (on average, 39.54 ± 3.01 N) although the actual force amplitude appeared to depend on stimulus type ($p < 0.01$) (Figure 5A). Similarly, the perturbation types in the constant-impulse series were well characterized by distinct force values and similar impulse values (on average, the impulse was equal to 4.60 ± 0.28 Ns) although a significant dependence of impulse on stimulus type was observed ($p < 0.01$) (Fig. 5B).

Note that, while impulse was precisely controlled among subjects, peak force exhibited some increased dispersion at 2 Ns compared to other impulse levels, possibly due to the difficulty in controlling short-duration perturbations.

In all subjects, ΔCoP exhibited a significant ($p<0.001$) and extremely good linear correlation with the impulse of the perturbation (Fig. 6A), $r = 0.96$ on average, in spite of the slight differences observed in average peak force levels. Conversely, the mean correlation between ΔCoP and force amplitude was poor ($r = 0.49$) and not statistically significant in 7 out of 14 subjects (Fig. 6B). The box plots of Fig. 6C show the distribution of the individual Pearson's correlation coefficients in the two cases.

The linearity of the relation between ΔCoP and impulse allowed normalizing the CoP displacement to the impulse of the perturbation: $\Delta CoP_n = \frac{\Delta CoP}{Impulse}$, which should then provide a postural index independent of the magnitude of perturbation (Dvir et al. 2020). This index remained fairly constant, within the constant-force series for impulse (range: 4-10 Ns). Friedman's ANOVA indicated a significant dependence of ΔCoP_n with impulse ($p < 0.01$) with a significantly increased value at impulse = 2 Ns compared to the other magnitudes ($p < 0.01$) (Fig. 7A). Also in the constant-impulse session, the experimental ΔCoP_n was influenced by the force amplitude of the perturbation ($p<0.01$) but only the response to F=100 N differed significantly from the other magnitudes (Fig. 7B): the ΔCoP_n at 100 N was significantly higher than the ΔCoP_n at 20 N ($p < 0.05$) and at 40 N ($p < 0.01$). Notably, on exclusion of the low-impulse (2 Ns) and high-force perturbations (100 N) the individual ΔCoP_n values remain fairly comparable, even in response to different stimulus types (ICC = 0.88 with 95% confident interval [0.75 – 0.96]). Furthermore, the normalized index ΔCoP_n showed relatively low variability when assessed in response to 5 perturbations of the same type: on average CoV = 13 ±7%.

A single index value was calculated for each subject by averaging the ΔCoP_n over all perturbations greater than 2 Ns and less than 100 N (mean [range]: 0.93 [0.72 – 1.15] cm/Ns). The mean value of the ΔCoP_n was significantly inversely correlated with the physical characteristics of the subjects: weight (r = -0.79), height (r = -0.69) and foot length (r = -0.63).

In order to exclude postural adjustments in preparation for back perturbations, the resting CoP was analyzed for possible variations during the test. No significant change in resting CoP was detected within any of the 2 session and of the 8 perturbation sequences.

3.2 Simulations results

The tuning of the model was performed to match the average experimental ΔCoP_n response of Fig. 7A (black line). The comparison between simulation results and experimental data, for each testing condition selected during the trials carried out on healthy subjects, is shown in Fig. 8.

It can be observed that, in the absence of sensory noise, simulated ΔCoP exhibited a linear trend with the impulse (Fig. 8A, blue line) whereas no dependence on the force amplitude (Fig. 8B) was found. Accordingly, ΔCoP_n remained extremely constant over the entire range of impulse and force amplitude (Fig. 8C and D).

With the addition of noise to the sensory feedback, both ΔCoP and ΔCoP_n increased in all conditions (Fig 8 A-D, red lines). While this effect was uniform for ΔCoP in all conditions, it was particularly marked at low impulse for ΔCoP_n, thus faithfully matching the experimental data at 2 Ns.

4. DISCUSSION

To the best of our knowledge, this is the first study in which force and impulse of the trunk perturbations have been systematically varied in order to investigate their differential effect on PR. The issue was addressed by challenging the balance of healthy subjects by means of a custom-built perturbator, which proved adequate to deliver accurately controlled stimuli, and by analyzing simulated responses based on a simple inverse pendulum model.

The findings support the hypothesis formulated on the basis of a previous observation, namely, that the displacement of the CoP is consistently and strongly correlated with impulse and not significantly correlated with the force amplitude of the perturbation. Furthermore, since the extracted ΔCoP_n was quite constant across the perturbation range, the applicability of this index as a synthetic descriptor of the individual postural performance was further amplified.

Although, as pointed out, the association between ΔCoP and the magnitude of the perturbation has been highlighted before, a clear *linear* relationship has been evidenced experimentally only in a handful of studies. Kim et al (2009) showed that ΔCoP was positively correlated with the peak force of perturbations applied to the high back, in apparent contrast with the present results. However, we speculate that the duration of the perturbations (which was not measured) was quite constant across the different subjects, which would make impulse and force amplitude proportionally related and thus, both correlated with ΔCoP. Our preliminary study on PR (Dvir et al. 2020) indicated a moderate correlation between ΔCoP and force ($r = 0.50$) and a stronger correlation with the impulse of the perturbation ($r = 0.71$)

but the distributions of the individual Pearson correlation coefficients were quite dispersed, possibly because the study was based on uncontrolled manually-delivered perturbations. The possibility to deliver accurate perturbations in the present study effectively reduced the intra-subject variability in the PR and revealed the clear-cut linear relationship between ΔCoP and impulse ($r = 0.96$) while confirming a low correlation between ΔCoP and force amplitude ($r = 0.49$ on average but reaching significance only in 7 subjects). Moreover, the reproducibility of the disturbances provided by the perturbator was adequate for the application, as signaled by the results shown in Fig. 5, confirming that the performance of the device was not significantly affected by the presence of a human operator (Ferraresi et al. 2020b; Maffiodo et al. 2020). Notably, as compared to our previous study based on manual uncontrolled perturbations, with the new perturbator we were able to reduce the within-subject variability of ΔCoP_n, from about 20 ± 8 % (recalculated from previous data) to 13 ± 7 %. As a result, it was here possible to achieve a comparable ICC with as few as 5 perturbations, instead of the 20 stimuli used in the previous study.

The results of the study reinforce the concept that a single index, ΔCoP_n, obtained from the ratio of ΔCoP and impulse, may synthetically describe the PR of the subject, independently of the magnitude of the perturbation (Dvir et al. 2020). In fact, this index is here shown to remain fairly constant in a wide range of force and impulse intensity (Fig. 7). Notably, this index was slightly but significantly increased at low impulse and high force amplitude: a pattern not predicted by the model (Fig. 8 D). While significant non-linearities are embedded in the postural control system, starting from the muscle level (Ivanenko and Gurfinkel 2018), the present deviation from linearity could be related to the short duration of the perturbation, which is below 75 ms for both 2 Ns and 100 N. In fact it has been proposed that short stimuli elicit a triggered response, uninfluenced by the stimulus characteristics, while a longer stimulus duration would be necessary for sensory inputs to encode the magnitude of the perturbation and help to shape a proportionate response (Diener et al. 1988). On the other hand, the results here obtained with the model also suggest that, at low perturbation magnitudes, the presence of noise in the system may account for a similar non-linearity (Fig 8 C-D).

While the implemented model completely excludes a dependence of the PR on the force amplitude, a significant correlation was evidenced in some subjects (Fig. 6B). It may be observed that these individual correlations are based on only 4 points and thus heavily depend on each single measurement. As a consequence, increased correlations would result due to the abnormally increased response at 100 N, as previously discussed. On the other hand, a weak correlation with the force amplitude could also result from the involvement of additional sensory feedback pathways, particularly sensitive to the force stimulus (e.g., touch receptors of the back, vestibular receptors), not included in the present model.

Regarding the accuracy of the simulations, the approach to model tuning used in this study was considered suitable to achieve a realistic although simplified behavior of the model, however it is well known that all the active and passive response parameters discussed are highly subject-specific and require accurate estimation when a detailed description of balance control is targeted (Goodworth and Peterka 2018).

5. LIMITATIONS

As a first approximation, the balance reaction of healthy young adults in response to low disturbance mainly consists of a correcting torque at the ankle (Horak and Nashner 1986; Shumway-Cook and Woollacott 2007). Therefore, a single-link inverted pendulum model was developed to simulate the postural response of the study participants. This approximation was supported by the visual inspection of the experimental trials, that confirmed how most oscillations occurred about the ankle joints. As indicated by the good match between experimental and simulated data, this simple model proved to be sufficiently accurate for the purpose of testing the relationship between the displacement of the CoP and the impulse of the perturbation. On the other hand, we cannot exclude that other postural strategies, such as the hip strategy, could also contribute to the whole response, particularly to high-magnitude perturbations. This would likely affect the correlation between ΔCoP_n and impulse, although the precise effects are difficult to predict, based on the present experiments. Appropriate integration of the hip strategy into the model requires to adopt a double-link inverted pendulum model, resulting in a far more complex optimization problem, with additional unknown control parameters used to model the correcting torque at the hip and the interaction between active controls at each joint (Goodworth and Peterka 2018). This, in turn, requires the acquisition of additional descriptors of the postural response, e.g. tangential forces at the platform, movements and acceleration of the different body segments. The present results suggest that this increase in complexity is not necessary for describing the response to small postural perturbation.

Another limitation of the study was the non-exactly constant value of the force amplitude and of the impulse in the force constant session and in the impulse constant session, respectively. The perturbations were applied to the subjects with a custom-made device consisting of a low friction pneumatic actuator controlled in force and position by a PI controller. The nonlinearities and relatively slow dynamics associated to pneumatic systems and the inertia of the piston make the PI controller not able to appropriately minimize the error between the force reference profile and the applied force in a very short time. As a result, there is an overshoot in the first 35 ms of the perturbation that impacts on the calculated Force Amplitude, especially in the case of short-lasting perturbations. To obtain more accurate perturbation profiles and more robust control, an electrically-actuated perturbator based on Model Predictive Control, with inherent high dynamics and stiffness, is currently under development (Pacheco Quiñones et al. 2021).

6. CONCLUSION

The results support the use of the impulse rather than the force as input variable in impulsive perturbations applied to the trunk. Thanks to the linearity of the relationship between ΔCoP and impulse, the postural index, ΔCoP_n, may be used as a synthetic descriptor of the individual postural performance.

CONFLICT OF INTEREST STATEMENT

The authors have no conflict to disclose.

ACKNOWLEDGMENTS

This work was supported by grants from "Fondo Europeo di sviluppo regionale – Regione Liguria" (ROAS_RIC_COMP_17_01) and by "Proof of Concept" Project 2018, the Politecnico di Torino. Funding sources had no role in the conduction of the study.

REFERENCES

Azzi NM, Coelho DB, Teixeira LA (2017) Automatic postural responses are generated according to feet orientation and perturbation magnitude. Gait Posture 57:172–176. doi: 10.1016/j.gaitpost.2017.06.003

Boonstra TA, Schouten AC, Van Der Kooij H (2013) Identification of the contribution of the ankle and hip joints to multi-segmental balance control. J Neuroeng Rehabil 10:23. doi: 10.1109/TNSRE.2014.2372172

Bortolami SB, DiZio P, Rabin E, Lackner JR (2003) Analysis of human postural responses to recoverable falls. Exp Brain Res 151:387–404. doi: 10.1007/s00221-003-1481-x

Chen B, Lee YJ, Aruin AS (2017) Role of point of application of perturbation in control of vertical posture. Exp Brain Res 235:3449–3457. doi: 10.1007/s00221-017-5069-2

Colebatch JG, Govender S (2019) Responses to anterior and posterior perturbations in Parkinson’s disease with early postural instability: role of axial and limb rigidity. Exp Brain Res 237:1853–1867. doi: https://doi.org/10.1007/s00221-019-05553-8

Colebatch JG, Govender S, Dennis DL (2016) Postural responses to anterior and posterior perturbations applied to the upper trunk of standing human subjects. Exp Brain Res 234:367–376. doi: 10.1007/s00221-015-4442-2

Diener HC, Horak FB, Nashner LM (1988) Influence of stimulus parameters on human postural responses. J Neurophysiol 59:1888–1905. doi: 10.1152/jn.1988.59.6.1888

Dvir Z, Paterna M, Quargnenti M, et al (2020) Linearity and repeatability of postural responses in relation to peak force and impulse of manually delivered perturbations : a preliminary study. Eur J Appl Physiol 120:1319–1330. doi: 10.1007/s00421-020-04364-y

Engelhart D, Schouten AC, Aarts RGKM, Van Der Kooij H (2015) Assessment of Multi-Joint Coordination and Adaptation in Standing Balance : A Novel Device and System Identification Technique. IEEE Trans Neural Syst Rehabil Eng 23:973–982. doi: 10.1109/TNSRE.2014.2372172

Ferraresi C, De Benedictis C, Muscolo GG, et al (2020a) Development of an Automatic Perturbator for Dynamic Posturographic Analysis. Mechanisms ans Machine Science 93:273–282. doi: 10.1007/978-3-030-58104-6

Ferraresi C, Maffiodo D, Franco W, et al (2020b) Hardware-In-the-Loop Equipment for the Development of an Automatic Perturbator for Clinical Evaluation of Human Balance Control. Appl Sci 10:8886. doi: 10.3390/app10248886

Forghani A, Preuss R, Milner TE (2017) Effects of amplitude and predictability of perturbations to the arm on anticipatory and reactionary muscle responses to maintain balance. J Electromyogr Kinesiol 35:30–39. doi: http://dx.doi.org/10.1016/j.jelekin.2017.05.006

Fujimoto M, Bair WN, Rogers MW (2015) Center of pressure control for balance maintenance during lateral waist-pull perturbations in older adults. J Biomech 48:963–968. doi: 10.1016/j.jbiomech.2015.02.012

Goodworth AD, Peterka RJ (2018) Identifying mechanisms of stance control : A single stimulus multiple output model-fit approach. J Neurosci Methods 296:44–56. doi: 10.1016/j.jneumeth.2017.12.015

Grassi L, Rossi S, Studer V, et al (2017) Quantification of postural stability in minimally disabled multiple sclerosis patients by means of dynamic posturography: An observational study. J Neuroeng Rehabil 14:4. doi: 10.1186/s12984-016-0216-8

Horak FB, Nashner LM (1986) Central programming of postural movements: adaptation to altered support-surface configurations. J Neurophysiol 55:1369–81. doi: 10.1152/jn.1986.55.6.1369

Ivanenko Y, Gurfinkel VS (2018) Human postural control. Front Neurosci 12:171. doi: 10.3389/fnins.2018.00171

Kim J, Kim C, Lee J, et al (2009) Human postural control against external force perturbation applied to the high-back. Int J Precis Eng Manuf 10:147–151. doi: 10.1007/s12541-009-0083-3

Kim S, Atkeson CG, Park S (2012) Perturbation-dependent selection of postural feedback gain and its scaling. J Biomech 45:1379–1386. doi: 10.1016/j.jbiomech.2012.03.001

Maaswinkel E, Griffioen M, Perez RSGM, van Dieën JH (2016) Methods for assessment of trunk stabilization, A systematic review. J Electromyogr Kinesiol 26:18–35. doi: 10.1016/j.jelekin.2015.12.010

Maffiodo D, Franco W, De Benedictis C, et al (2020) Pneumo-tronic Perturbator for the Study of Human Postural Responses. Advances in Intelligent Systems and Computing 980:374–383. doi: 10.1007/978-3-030-19648-6_43

Martinelli AR, Coelho DB, Magalhães FH, et al (2015) Light touch modulates balance recovery following perturbation: from fast response to stance restabilization. Exp Brain Res 233:1399–1408. doi: 10.1007/s00221-015-4214-z

Morasso PG, Baratto L, Capra R, Spada G (1999) Internal models in the control of posture. Neural Networks 12:1173–1180. doi: 10.1016/S0893-6080(99)00058-1

Pacheco Quiñones D, Paterna M, De Benedictis C (2021) Automatic electromechanical perturbator for postural control analysis based on model predictive control. Appl Sci 11:4090. doi: 10.3390/app11094090

Pasman EP, McKeown MJ, Cleworth TW, et al (2019) A novel MRI compatible balance simulator to detect postural instability in parkinson's disease. Front Neurol 10:922. doi: 10.3389/fneur.2019.00922

Pidcoe PE, Rogers MW (1998) A closed-loop stepper motor waist-pull system for inducing protective stepping in humans. J Biomech 31:377–381. doi:

10.1016/S0021-9290(98)00017-7

Robbins SM, Caplan RM, Aponte DI, St-Onge N (2017) Test-retest reliability of a balance testing protocol with external perturbations in young healthy adults. Gait Posture 58:433–439. doi: 10.1016/j.gaitpost.2017.09.007

Robert T, Vallee P, Tisserand R (2018) Stepping boundary of external force-controlled perturbations of varying durations : Comparison of experimental data and model simulations. J Biomech 75:89–95. doi: 10.1016/j.jbiomech.2018.05.010

Schmidt D, Germano AMC, Milani TL (2015) Aspects of dynamic balance responses: Inter- and intra-day reliability. PLoS One 10:e0136551. doi: http://dx.doi.org/10.1371/journal.pone.0136551

Shumway-Cook A, Woollacott MH (2007) Motor Control: Translating research into clinical practice, 3rd edn. Lippincott Williams & Wilkins, Philadelphia, Pa, USA.

Sturnieks DL, Menant J, Delbaere K, et al (2013) Force-Controlled Balance Perturbations Associated with Falls in Older People: A Prospective Cohort Study. PLoS One 8:e70981. doi: 10.1371/journal.pone.0070981

Teixeira LA, Azzi N, de Oliveira JÁ, et al (2019) Automatic postural responses are scaled from the association between online feedback and feedforward control. Eur J Neurosci 1–10. doi: 10.1111/ejn.14625

Van Der Kooij H, Peterka RJ (2011) Non-linear stimulus-response behavior of the human stance control system is predicted by optimization of a system with sensory and motor noise. J Comput Neurosci 30:759–778. doi: 10.1007/s10827-010-0291-y

Van Der Kooij H, Van Asseldonk E, Van Der Helm FCT (2005) Comparison of different methods to identify and quantify balance control. J Neurosci Methods 145:175–203. doi: 10.1016/j.jneumeth.2005.01.003

Winter DA, Patla AE, Prince F, et al (1998) Stiffness control of balance in quiet standing. J Neurophysiol 80:1211–1221. doi: 10.1152/jn.1998.80.3.1211

FIGURE LEGENDS

Figure 1. Experimental Set-up. A: pneumo-tronic perturbator, 1: low friction pneumatic actuator, 2: flow-proportional valves, 3: laser sensor, 4: load cell, 5: end striker, 6: handles, 7: trigger button. B: Example of experimental task with the operator handling the pneumo-tronic perturbator.

Figure 2. Force profiles for the different perturbation types included in the constant force series (A) and the constant impulse series (B). The intended force profile (red) is superimposed to the actually delivered force profile (blue, average across all subjects).

Figure 3. A representative recording of the perturbation (Black line) and the ensuing displacement of the Center of Pressure (dashed grey line) observed

during experimentation (constant-force series: 40 N, 6 Ns).

Figure 4. Free body diagram of a single-link inverted pendulum model for postural control analysis. θ is the body oscillation, l is the height of the subject with respect to the ankle joint; h_F is the distance between ankle joint and the point of application of the perturbation force F_e; d is the distance between ankle joint and the center of mass (CoM); h is the height of ankle joint with respect to the fixed base of support; I is the rotational inertia of the body about the CoM; m is the subject body mass; $\ddot{x}$ is the horizontal acceleration of the CoM; $\ddot{y}$ is the vertical acceleration of the CoM; $\ddot{\theta}$ is the angular acceleration of the CoM; g is the gravitational acceleration; τ is the correcting torque at the ankle; CoP is the center of pressure position; R_x is the horizontal component of the ground reaction force; R_y is the vertical component of the ground reaction force

Figure 5. Characteristics of delivered perturbations for the constant-force series (left) and the constant-impulse series (right). Each box represents the median and the standard deviation of the perturbations applied to the subjects (n=5 perturbation x 14 subjects = 70), for each stimulus type.

Figure 6. The relationship between the maximum displacement of the center of foot pressure, ΔCoP, and the magnitude of the perturbations, in terms of impulse (A) and force amplitude (B) for each participant in the experimental trial. Distribution of the Pearson's Correlation Coefficients, for the ΔCoP – Impulse (Black) and the ΔCoP - Force (white) correlation (C).

Figure 7. The relationship between the postural index ΔCoP_n and the magnitude of perturbation expressed in terms of impulse (A) and force amplitude (B) for each participant in the experimental trial (colored line). The thick black line represents the average trend.

Figure 8 The relationship between the simulated maximum displacement of the center of foot pressure, ΔCoP, and the magnitude of the perturbations, in terms of impulse (A) and force amplitude (B). The relationship between the postural index ΔCoP_n and the magnitude of perturbation expressed in terms of impulse (C) and force amplitude (D).

Red lines refer to the results of the simulation performed considering the sensorial noise; blue lines refer to the results of the simulation performed without the contribution of the sensorial noise; black lines are the average experimental trend calculated on all the participants of the experimental analyses**.**

599

A B

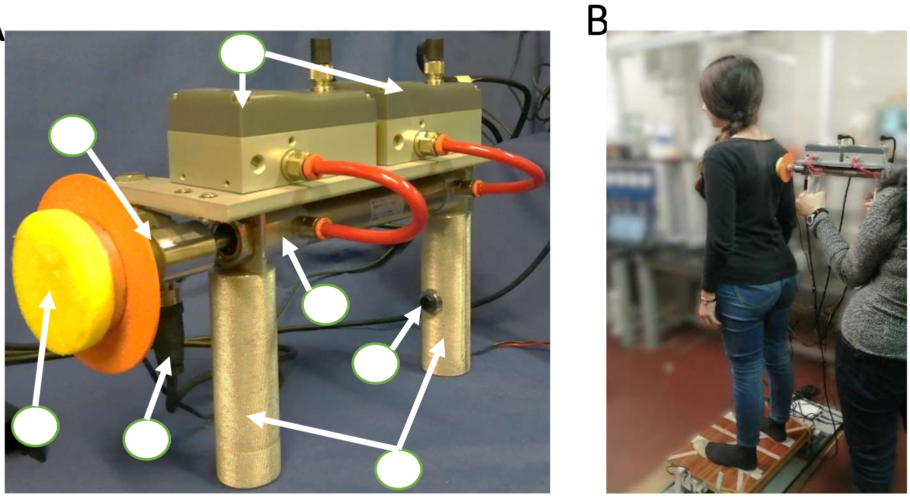

Figure 1

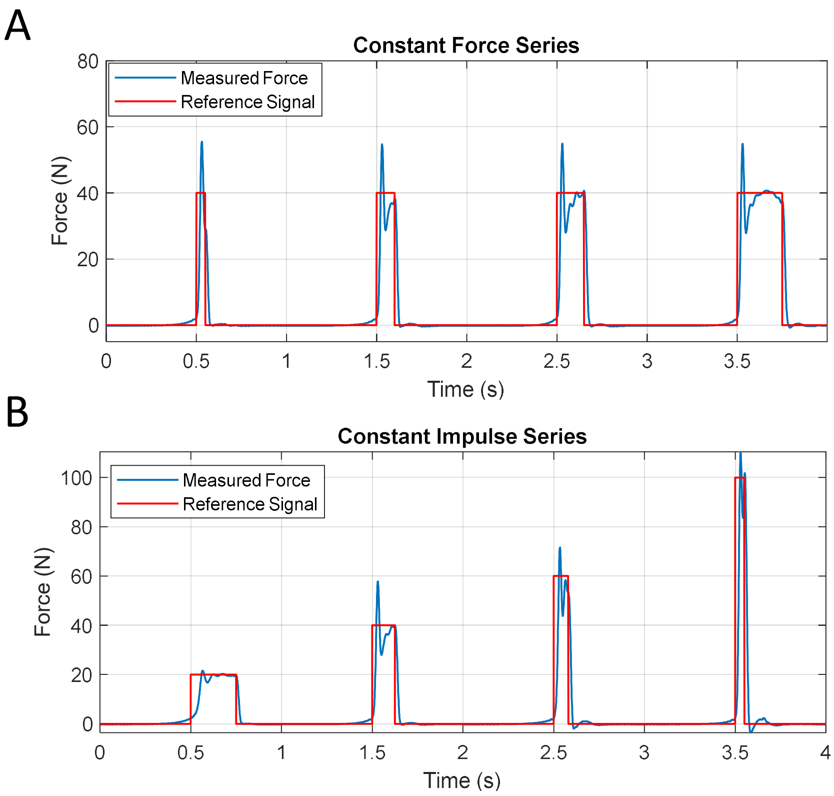
A
Constant Force Series
Measured Force
Reference Signal
Force (N)
Time (s)
B
Constant Impulse Series
Measured Force
Reference Signal
Force (N)
Time (s)

Figure 2

602

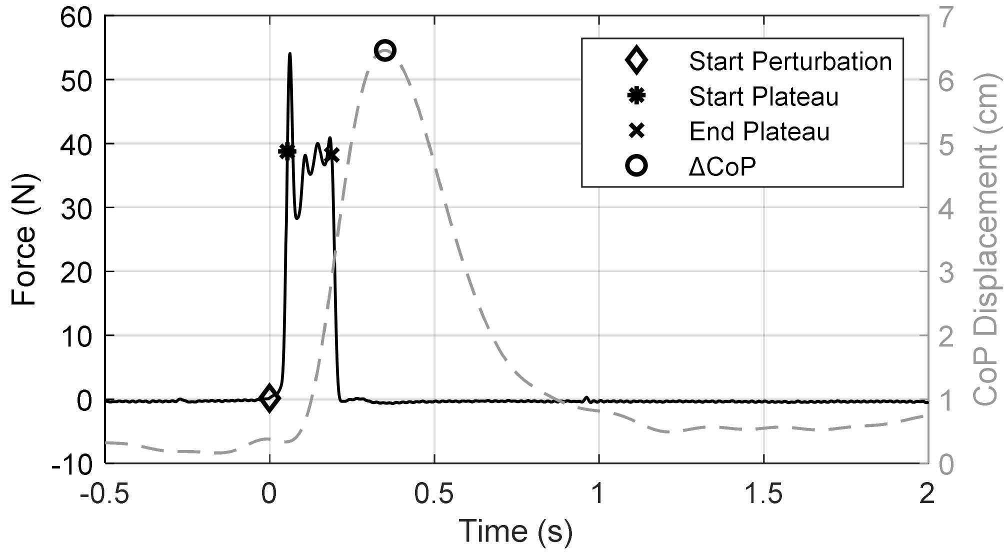

60
50
40
30
20
10
0
-10
Force (N)
7
6
5
4
3
2
1
0
CoP Displacement (cm)
-0.5
0
0.5
1
1.5
2
Time (s)
Start Perturbation
Start Plateau
End Plateau
ΔCoP

Figure 3

603

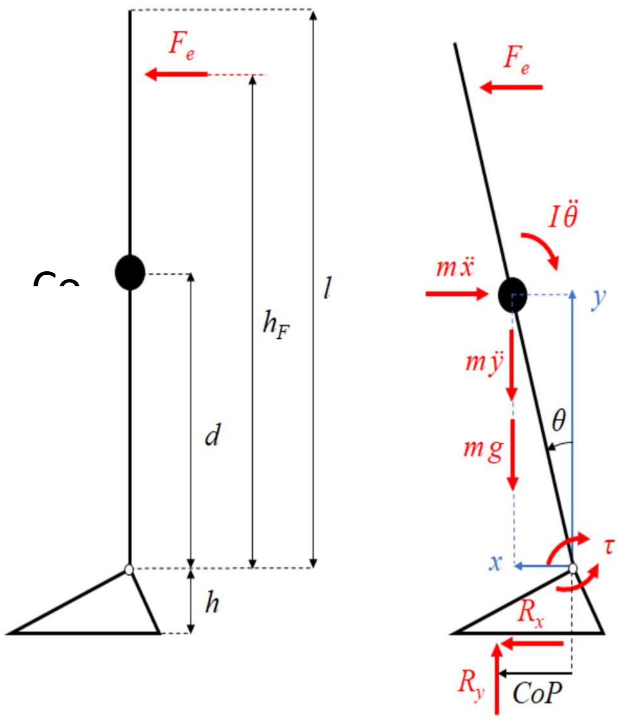

F_e
h_F
l
d
h
F_e
$I\ddot{\theta}$
$m\ddot{x}$
y
$m\ddot{y}$
θ
mg
τ
x
R_x
R_y
CoP

Figure 4

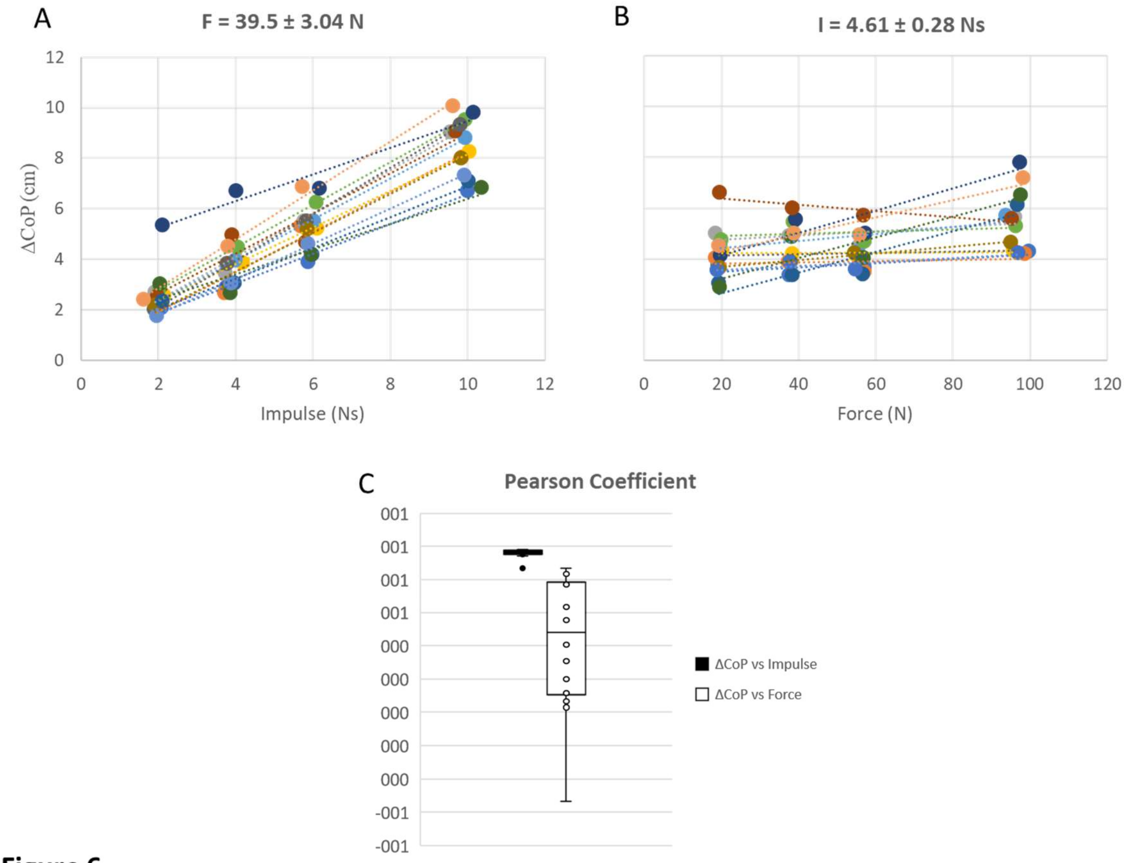
A
F = 39.5 ± 3.04 N
ΔCoP (cm)
Impulse (Ns)
B
I = 4.61 ± 0.28 Ns
Force (N)
C
Pearson Coefficient
ΔCoP vs Impulse
ΔCoP vs Force

Figure 6

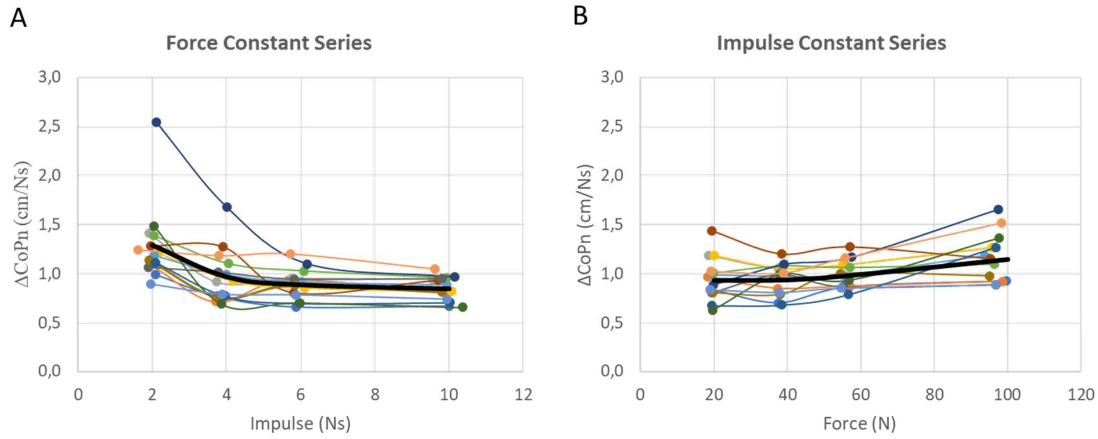
A
Force Constant Series
ΔCoPn (cm/Ns)
Impulse (Ns)
B
Impulse Constant Series
ΔCoPn (cm/Ns)
Force (N)

Figure 7

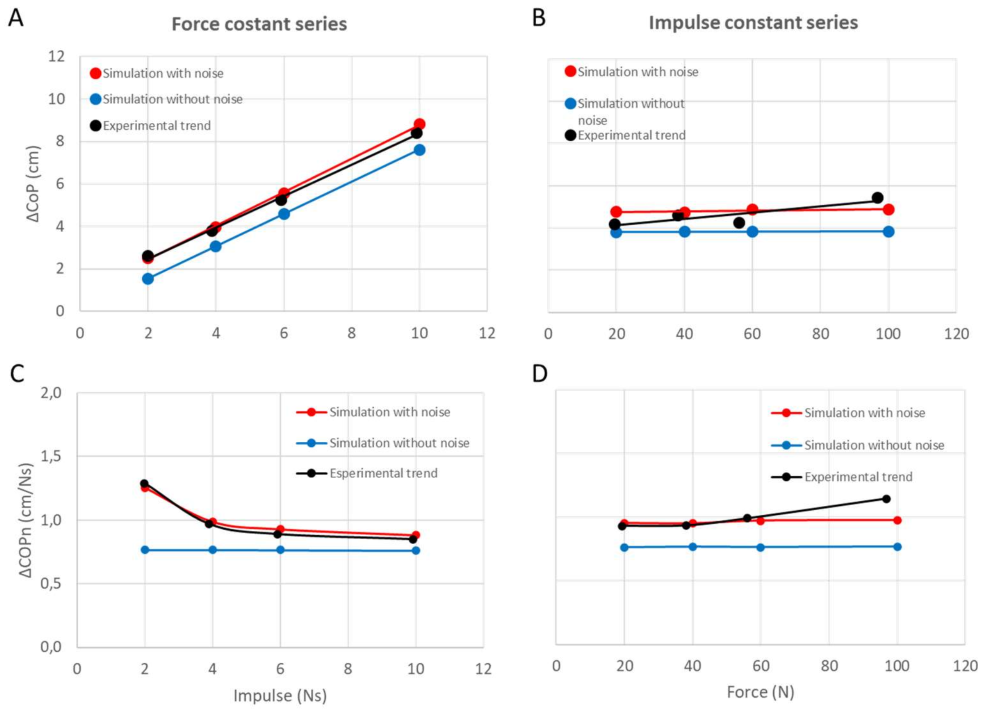
A
Force costant series
12
10
8
6
4
2
0
ΔCoP (cm)
Simulation with noise
Simulation without noise
Experimental trend
0 2 4 6 8 10 12
B
Impulse constant series
Simulation with noise
Simulation without noise
Experimental trend
0 20 40 60 80 100 120
C
2,0
1,5
1,0
0,5
0,0
ΔCOPn (cm/Ns)
Simulation with noise
Simulation without noise
Esperimental trend
0 2 4 6 8 10 12
Impulse (Ns)
D
Simulation with noise
Simulation without noise
Experimental trend
0 20 40 60 80 100 120
Force (N)

606 **Figure 8**